Supporting Information for

Dynamic Nuclear Polarization Based on an Endogenous Radical

Thorsten Maly, Dongtao Cui, Robert G. Griffin and Anne-Frances Miller *

[1] Francis Bitter Magnet Laboratory and Department of Chemistry, Massachusetts Institute of Technology, Cambridge, MA 02139 (USA), [2] Department of Chemistry, University of Kentucky Lexington, KY 40506-0055 (USA).

* Corresponding author: Anne-Frances Miller: afm@uky.edu, tel: (859) 257-9349.

Figure S1: 9 GHz (X-band) EPR signal of the FD SQ radical

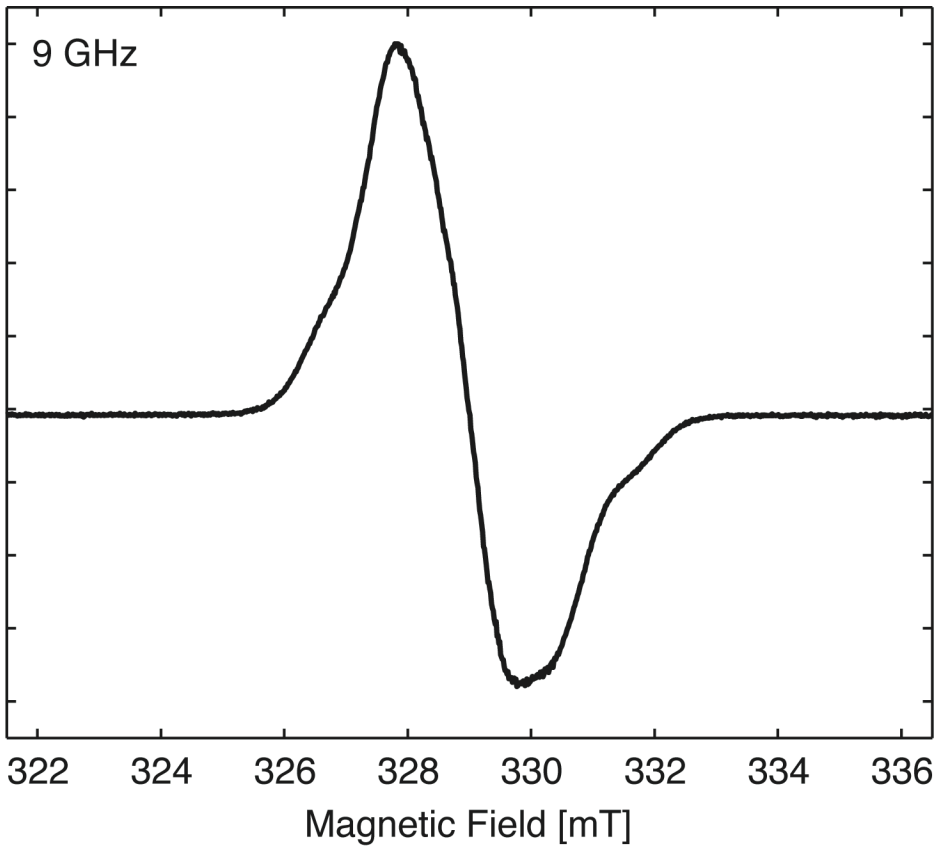

Figure S1: 9 GHz cw EPR spectrum of the FD semiquinone. Experimental parameters : temperature 20 K, microwave frequency 9.3353 GHz (uncalibrated), microwave power 0.2 mW, modulation amplitude 0.05 mT, modulation frequency 100 kHz, 1 scan.

Figure S2: 140 GHz EPR Signal and Simulation

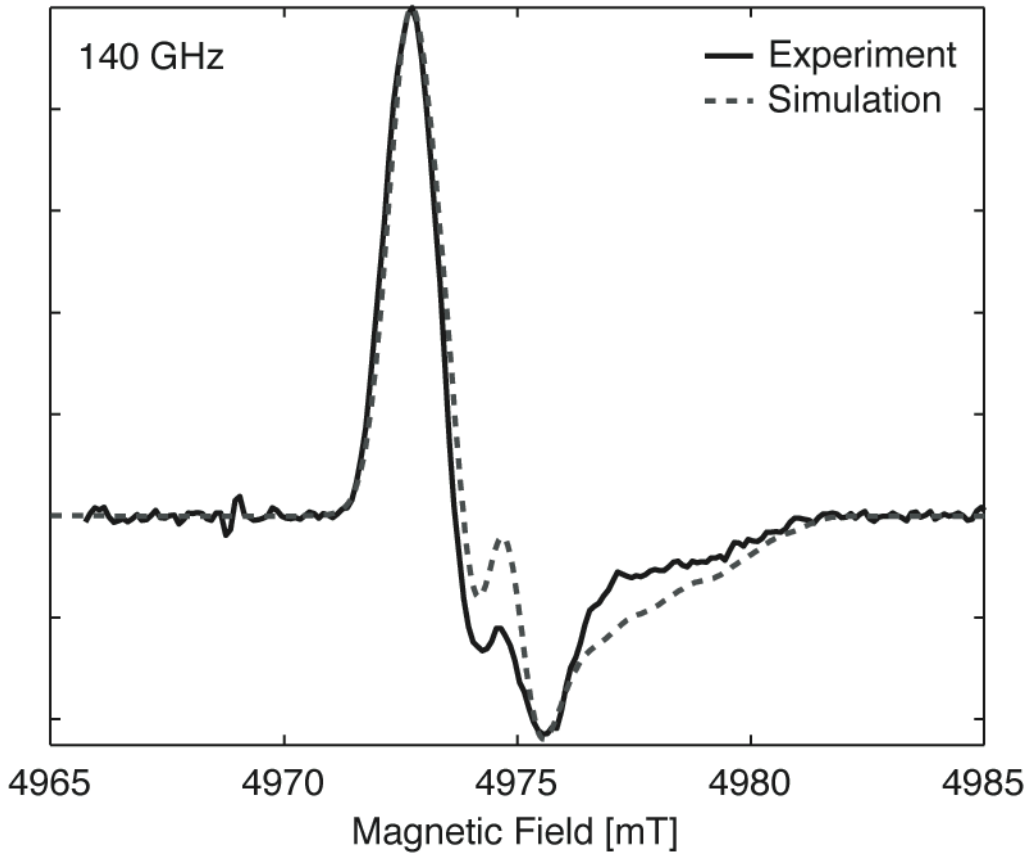

Figure S2: 140 GHz pulsed EPR spectrum of FD SQ in $^{2}H_{8}$-glycerol/$^{2}H_{2}O$ buffer (60:50, v:v) taken at 40 K. The pseudo-modulated spectrum was calculated using a modulation amplitude of 0.3 mT (solid line). The spectrum is identical to that shown in Figure 3 in the manuscript. The simulation of the spectrum is shown as dashed line. Details are given below.

Simulation of the 140 GHz EPR spectrum were performed using the EasySpin simulation software for Matlab [1]. The following simulation parameters were used: g_{xx} = 2.00431, g_{yy} = 2.00360, g_{zz} = 2.00217, Γ = [0.73 0.94 1.2] mT (inhomogenous linewidth), Hyperfine couplings: N5: $A_{||}$ = -0.06 mT, $A_{\perp}$ = 1.53 mT, N10: $A_{||}$ = 0.04 mT, $A_{\perp}$ = 0.83 mT, H5: A_{xx} = -0.3 mT, A_{yy} = -1.33 mT, A_{zz} = -0.89 mT. Simulation parameters are taken from [2].

A satisfying match of the simulation with the experimental spectrum could be achieved using the parameters of Schnegg et al [2] without any changes. All spectral features are reproduced and differences between the simulation and the experimental spectrum most likely arise from different linewidths. Further optimization of the simulations parameters is beyond the scope of this manuscript.

Figure S3: Power dependence of SQ-based DNP on ^{1}H-FD

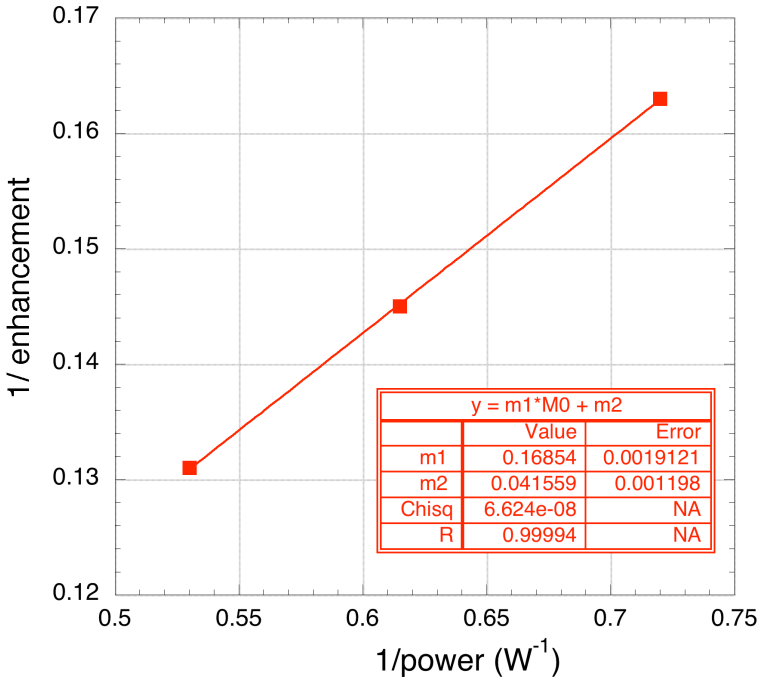

Figure S3: Observed power dependence of the SE DNP based on SQ radicals in ^{1}H-FD.

The power dependence of DNP is described by $\frac{1}{\varepsilon_\infty} = \frac{1}{\varepsilon_{max}}(1 + \frac{1}{aP})$ where ε_∞ is the steady-state enhancement obtained at $t_{mw} \rightarrow \infty$, ε_{max} is the enhancement at infinite power and a is the saturation factor which depends on the EPR relaxation properties of the polarizing agent.

Thus $1/\varepsilon_{max}$ is the intercept and $1/(a\varepsilon_{max})$ is the slope of a plot of $1/\varepsilon_\infty$ vs. 1/P. While only three data points were obtained for this sample, power dependencies for other samples were linear over 7 points and the three obtained here give no indication of non-linearity. Based on our intercept ε_{max} is 1/.04 = 25.

Table S1: Total number of ^{1}H and ^{13}C atoms in FD

The number of each amino acid in FD is used with the number of H and C atoms in each amino acid to calculate the total number of H and C atoms in the protein. The contributions of bound FMN are added to that. The calculation also takes into account loss of one H_2O per peptide linkage formed as well as the LEH_6 tag added to the C-terminus and conversion of a P to an A at the second position, as part of our cloning strategy.

Residue	A	R	N	D	C	E	Q	G	H	I	L	K	M	F	P[a]	S	T	W	V	Y
No. AA	17	7	2	17	4	13	3	18	1	0	12	4	0	6	2	8	7	2	9	5
His tag	1								6		1									
^{13}C/Res	3	6	4	4	3	5	5	2	6	6	6	6	5	9	5	3	4	11	5	9
^{1}H/Res	7	14	8	7	7	9	10	5	9	13	13	14	11	11	9	7	9	12	11	11
Total ^{1}H	126	98	16	119	28	126	30	90	63	0	169	56	0	66	27	56	63	24	99	55
Total ^{13}C	54	42	8	68	12	70	15	36	42	0	78	24	0	54	15	24	28	22	45	45

290 ^{1}H nuclei (corresponding to 145 H_2O molecules) were subtracted to account for peptide linkages. 21 ^{1}H and 15 C were added for the FMN. 143 backbone amides were considered to retain substantially proteated despite our use of deuterated medium because the FD amides exchange very slowly, on a timescale of days, we maintain the samples at 4 °C during all handling and only 1.5 days were needed complete exchange of the medium, reduction to the SQ state and freezing. Exchangeable H from the side chains of D, E, K S, T and Y are considered to have been lost (62).

Total number of 1H nuclei: **1302 – 290 + 21-62 = 969**

Total number of ^{13}C nuclei: **677 + 15 = 692**

^{1}H Concentrations

Buffer

The buffer was prepared from d_8-glycerol and D_2O at a ratio of 70/30 (v/v). The ^{1}H concentration in the medium was calculated to be 0.8 M assuming 99 % of deuteration for d_8-Glycerol and 99.9 % for D_2O.

Flavodoxin

From Watt et al., the molecular volume for Flavodoxin is 18,200 Å^3 (oxidized, room temperature) [3]. Using a molecular volume of 18.2 nm^3 per molecule and a total of 969 protons per molecule a ^{1}H concentration of 88 M can be calculated (969/(18.2e-24 * N_A)).

At 85 % deuteration the 1H concentration is reduced to 13 M

Average ^{1}H-^{1}H distances

Based on the knowledge of the ^{1}H concentration an average distance between ^{1}H nuclei can be calculated assuming a body-centered cubic packing:

$$r = \frac{\sqrt{3}}{2}\sqrt[3]{\frac{2}{N_A c}}$$

with r the distance, c the concentration and N_A the Avogadro number. The following distances were calculated:

Buffer	(0.8 M)	r = 1.4 nm
^{1}H-FD	(88 M)	r = 0.29 nm
^{2}H-FD	(13 M)	r = 0.55 nm

^{1}H-to-SQ and ^{1}H-to-Surface Distances in Flavodoxin

To calculate distances between protons in FD and the SQ radical, and distances between protons and the nearest TOTAPOL molecule, we took advantage of the high structural homology among flavodoxins from *D. vulgaris* (coordinate set 4FX2.pdb [3]) and *E. coli* (coordinate set 2HNB.pdb [4]). The former is a crystal structure providing locations for water molecules surrounding the FD molecule, whereas the latter is an NMR structure providing coordinates for all the ^{1}H atoms in FD. The two structures differ slightly with respect to the structure of surface loops but nonetheless share backbone rmsd of 1.36 Å (Figure S4A). This is adequate for our purpose, to simply estimate the distances of closest approach between the ^{1}H we observed, and each of SQ- or external TOTAPOL.

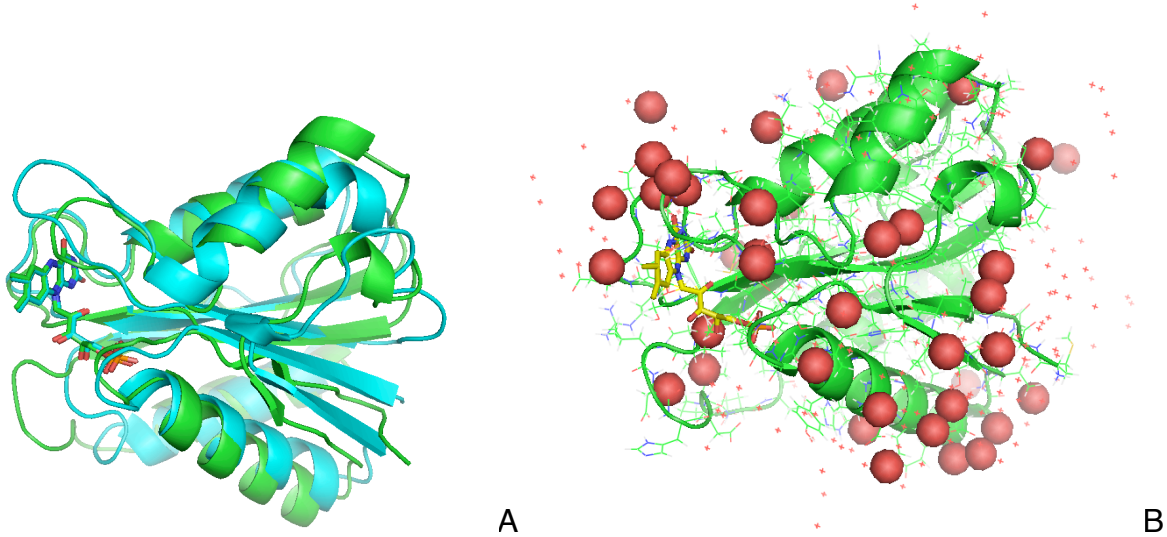

A B

Figure S4: A: overlay of the FD structure from *D. vulgaris* (aqua) and the MioC FD from *E. coli* (green) based on coordinate files 4FX2.pdb [3] and 2HNB.pdb model 21 [4], respectively. **B**: locations of water molecules surrounding FD 4FX2.pdb shown with the ribbon structure of model 21 of 2HNB.pdb after overlaying the latter on the 4FX2 structure (A). Water molecules with occupancies ≥ 0.8 are shown as red spheres and other water molecules as small red crosses. Figures were generated with Pymol [5].

The coordinates of model 21 of 2HNB.pdb were overlain on those of 4FX2.pdb using the 'fit' tools in Swiss PdbViewer (http://www.expasy.org/spdbv/). The position of

the flavin was approximated to be the centre of the central ring, determined by calculating the average of the coordinates of the six atoms of the central ring: C4a, N5, C5a, C9a, N10 C10a. To estimate the distribution of distances to FD's surface, all water molecules with occupancies of ≥ 0.8 from the 4FX2.pdb coordinate set were added to the 2HNB2 coordinate set produced by overlaying the two FDs, as the coordinates of their O atoms (red spheres in **Figure S4B**). Because some patches of the FD surface do not have high-occupancy waters, our criterion could produce longer-than-actual distances to the nearest H_2O, but such an error would tend to reproduce the longer distance of closest approach expected of a larger molecule such as TOTAPOL.

For each FD ^{1}H atom the distance to the center of the flavin and the distance to each of the high-occupancy water molecules was calculated. For each ^{1}H, the minimum distance to a water molecule was determined and rounded to the nearest integer, as was the distance to the flavin center. The number of protons at a given distance was plotted vs. the distance, to produce the distance distribution given in **Figure 6** for each of distance to the centre of the flavin and distance to the closest high-occupancy water. The average distance to the closest high-occupancy water is 6.3 Å, the standard deviation of the distribution is 2.5 Å, and the mode of the distribution is 5 Å. The average distance to the centre of the flavin is 20.7 Å, the standard deviation of this distribution is 7.9, Å, and the mode of this distribution is 26 Å. Data from a total of 1081 ^{1}Hs are presented.

Figure S5:

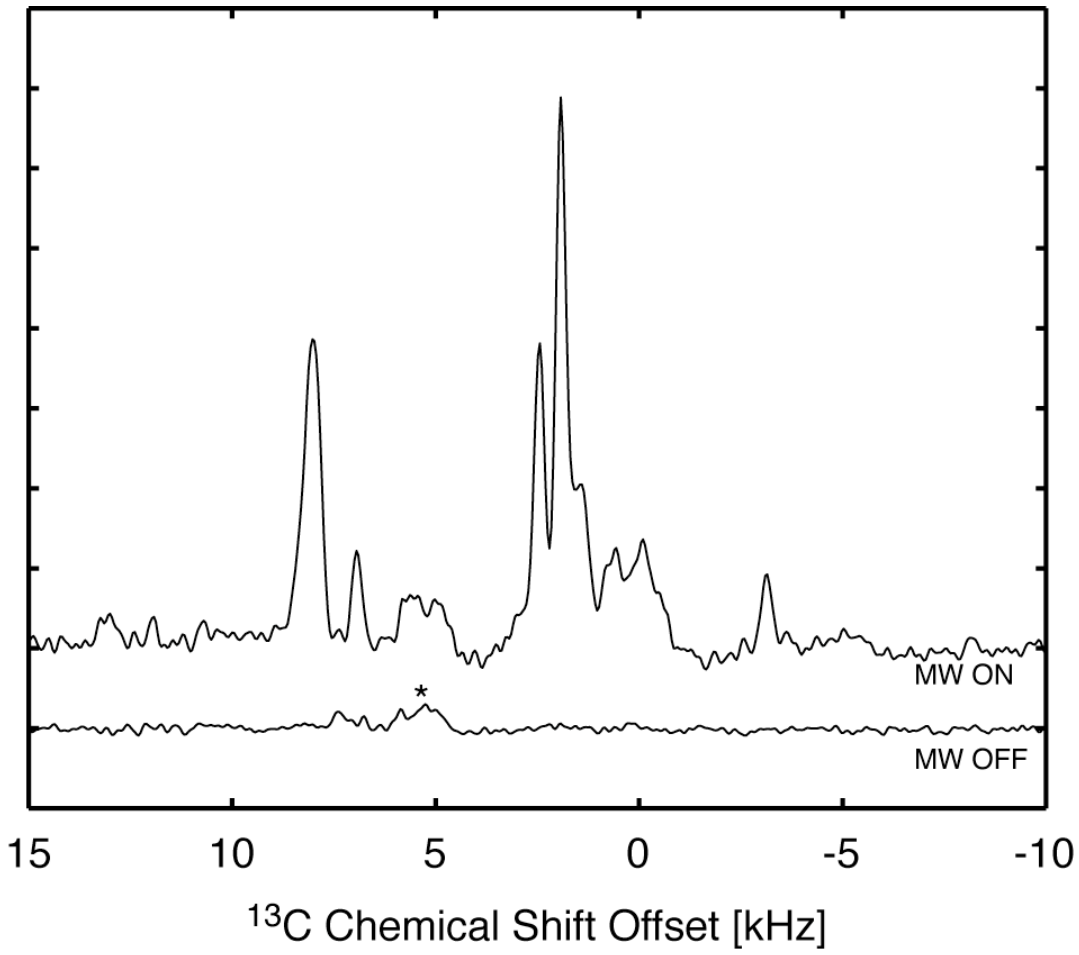

Figure S5: ^{1}H-DNP-enhanced ^{13}C spectrum of U-^{13}C FD using the exogenous polarizing agent TOTAPOL. The estimated enhancement is $\varepsilon > 100$. The signals observed in the MW OFF spectrum are ^{13}C impurities from the stator. The ^{1}H polarization is transferred to ^{13}C nuclei using a 0.7 ms cross-polarization step. Acquisition of the ^{13}C signal is performed under ^{1}H TPPM decoupling. The microwave polarization time was 20s and the spinning frequency was set to 5 kHz. Sample temperature: 90 K.

Figure S6: Comparison of buildup curves obtained via ^{1}H vs. ^{13}C detection

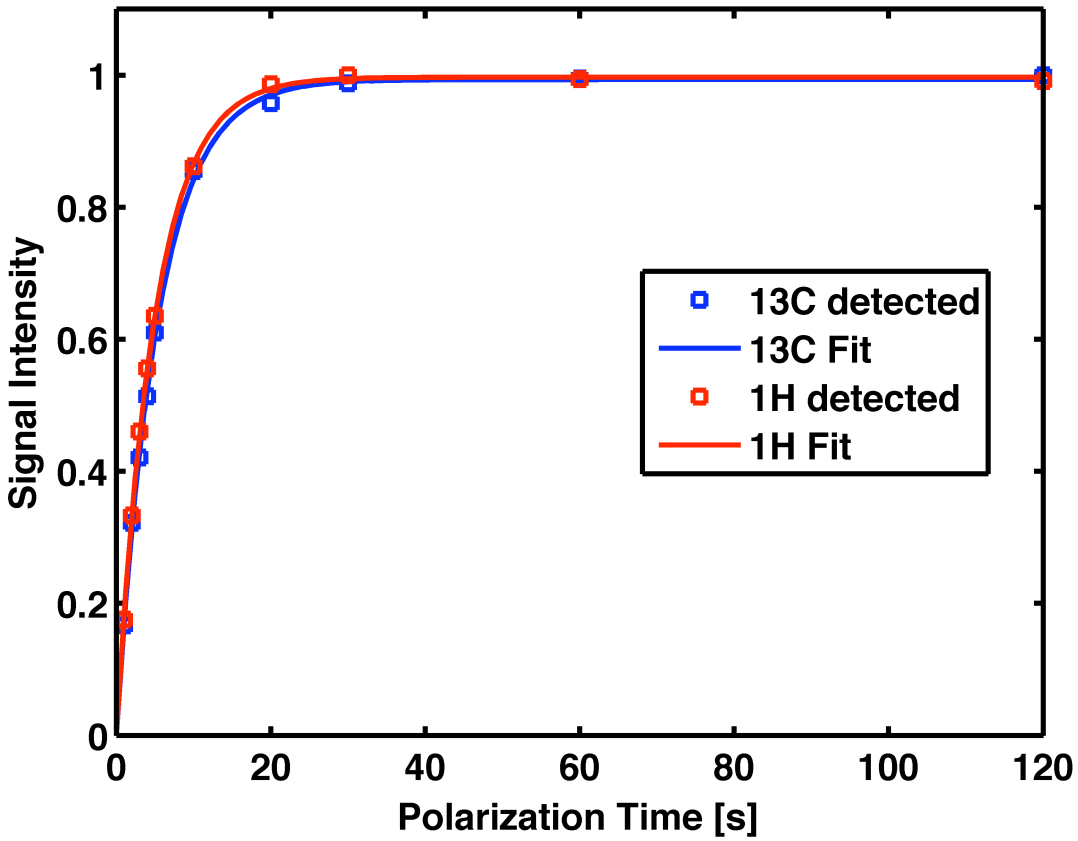

Figure S6: Comparison of direct ^{1}H detection and indirect ^{1}H detection through a CP step to ^{13}C. Sample was [^{2}H,^{13}C]-FD and the polarization agent was 10 mM TOTAPOL.

Both traces can be fitted using a mono-exponential recovery function of the form $y(t) = 1-\exp(-t/\tau_B)$. Data shown here are already scaled by the steady state enhancement to facilitate visual comparison of the buildup kinetics. For both detection methods a build-up time of 5 s was determined.

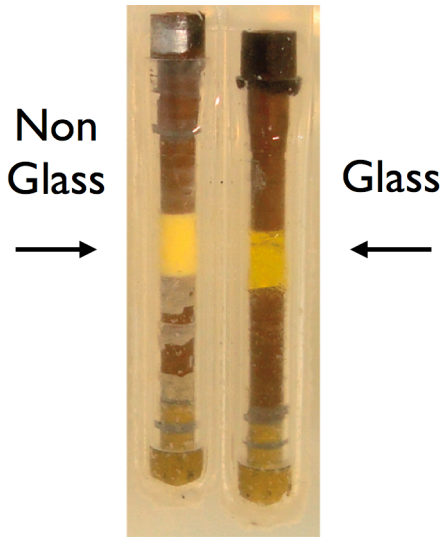

Figure S7: Comparison of a glassy sample (70% ^{2}H-glycerol: 30% $^{2}H_2O$ v:v) and a non-glass sample (12% ^{2}H-glycerol: 88% $^{2}H_2O$ v:v). Both contain 2 mM oxidized ^{1}H-FD and 10 mM TOTAPOL.

References for supplementary material

(1) Stoll, S.; Schweiger, A. *J Magn Reson* **2006**, *178*, 42-55.
(2) Schnegg, A.; Kay, C.; Schleicher, E.; Hitomi, K.; Todo, T.; Mobius, K.; Weber, A. *Mol. Phys.* **2006**, *104* 1627-1633.
(3) Watt, W.; Tulinsky, A.; Swenson, R. P.; Watenpaugh, K. D. *J Mol Biol* **1991**, *218*, 195-208.
(4) Hu, Y.; Li, Y.; Zhang, X.; Guo, X.; Xia, B.; Jin, C. *J. Biol. Chem.* **2006**, *281*, 35454-35466.
(5) DeLano, W. L. *http://www.pymol.org* **2002**, *DeLano Scientific*.

References for main manuscript with full authorship listed

(1) Maly, T.; Debelouchina, G. T.; Bajaj, V. S.; Hu, K.-N.; Joo, C.-G.; MakJurkauskas, M. L.; Sirigiri, J. R.; van der Wel, P. C. A.; Herzfeld, J.; Temkin, R. J.; Griffin, R. G. *J. Chem. Phys.* **2008**, *128*, 052211-052219.

(2) Barnes, A. B.; De Paëpe, G.; van der Wel, P. C. A.; Hu, K. N.; Joo, C. G.; Bajaj, V. S.; Mak-Jurkauskas, M. L.; Sirigiri, J. R.; Herzfeld, J.; Temkin, R. J.; Griffin, R. G. *Appl. Magn. Reson.* **2008**, *34*, 237-263.

(12) Barnes, A.; Corzilius, B.; Mak-Jurkauskas, M. L.; Andreas, L. B.; Bajaj, V. S.; Matsuki, Y.; Belenky, M.; Lugtenburg, J.; Sirigiri, J. R.; Temkin, R. J.; Herzfeld, J.; Griffin, R. G. *Phys. Chem. Chem. Phys.* **2010**, *12*, 5861-5867.

(15) Calle, C.; Sreekanth, A.; Fedin, M. V.; Forrer, J.; Garcia-Rubio, I.; Gromov, I.; Hinderberger, D.; Kasumaj, B.; Leger, P.; Mancosu, B.; Mitriakis, G.; Santangelo, M. G.; Stoll, S.; Schweiger, A.; Tschaggelar, R.; Harmer, J. *Helvetica Chimica Acta* **2006**, *89*, 2495-2521.

(74) Matsuki, Y.; Maly, T.; Ouari, O.; Karoui, H.; Moigne Le, F.; Rizzato, E.; Lyubenova, S.; Herzfeld, J.; Prisner, T. F.; Tordo, P.; Griffin, R. G. *Angew. Chem. Int. Ed.* **2009**, *48*, 4996-5000.

(75) Rosay, M.; Tometich, L.; Pawsey, S.; Bader, R.; Schauwecker, R.; Blank, M.; Borchard, P. M.; Cauffman, S. R.; Felch, K. L.; Weber, R. T.; Temkin, R. J.; Griffin, R. G.; Maas, W. E. *Phys. Chem. Chem. Phys.* **2010**, *12*, 5850-5860.